Probabilistic description of particle transport. II. Analysis of low-energy electron transmission through thin solid Xe and N_2 films

E. Keszei,* T. Goulet, and J.-P. Jay-Gerin†
Département de Médecine Nucléaire et de Radiobiologie, Faculté de Médecine, Université de Sherbrooke, Sherbrooke, Québec, Canada J1H 5N4
(Received 30 June 1987)

The probabilistic description of quasielastic particle transport given in a previous paper is used to analyze the results of low-energy electron transmission experiments on thin solid xenon and molecular nitrogen films deposited on a metal substrate. Values of the entrance probabilities of the incident electrons at the vacuum-film interface and of the electron scattering mean free paths in the films are extracted in the electron energy range 1.6–7.9 eV for xenon, and 2.4–7.4 eV for molecular nitrogen. The effects of anisotropy in the surface scattering and in the reflections at the two interfaces of the films are also discussed.

I. INTRODUCTION

In the preceding paper,[1] hereafter referred to as I, we presented a probabilistic model of quasielastic particle transport in plane-parallel media. This model is the first to account for both multiple scattering and the three-dimensional nature of the problem. Here, we show an important application of this model to the analysis of experimental low-energy (<20 eV) electron transmission (LEET) data on thin insulator films deposited on a metal substrate. This application was suggested by the increasing experimental and theoretical interest in LEET spectroscopy over the last decade.[2–20] A preliminary account of the present results has already been reported.[21]

Since our model deals only with quasielastic scattering processes, we have chosen in this study to analyze the experimental results for two materials which have considerably large energy regions (0–8 eV for solid xenon[7,10] and 2.5–7 eV for solid molecular nitrogen[16]) where electrons undergo elastic or quasielastic scattering exclusively. Each of these experiments has previously been reported and analyzed.[7,10,16] However, by comparing our results with those of the previous analyses, the significance of including both multiple scattering and a three-dimensional description of electron transport becomes apparent. Moreover, the flexibility of such a description allows us to discuss the effects of anisotropy in the surface scattering and in the reflections at the two interfaces of the films.

II. EXPERIMENT

The experimental method of LEET spectroscopy has been described in detail elsewhere.[5,7,16] In essence, a well-collimated monochromatic electron beam is incident perpendicularly from ultrahigh vacuum on a thin solid film grown *in situ* on a cold metallic substrate from the vapor of the studied molecules. The electron current I_t transmitted through the film to the metal is recorded for different film thicknesses as a function of the incident electron energy E (relative to the vacuum level). The incident current I_0 can be measured by retarding reflected electrons with deflector plates and returning them to the metal substrate.[5] The experiment thus provides a quantitative determination of the overall transmission coefficient of the film which is given by the ratio I_t/I_0.

The LEET spectra that we analyze in this paper were obtained with films of various thicknesses. For solid xenon films, the data consist of 16 different overlayer coverages between 4 and 500 monolayers,[7,10] a monolayer of solid xenon being approximately 0.354 nm thick.[10] In the case of solid molecular nitrogen, only 7 different overlayer thicknesses are available for analysis. They range from 3 to 20 monolayers, with an interlayer spacing of about 0.326 nm.[16] In both cases, the metal substrate was a polycrystalline platinum sheet with a (111) surface orientation, and the electron energy range covered was 0–20 eV.

III. THEORY

In I, we derived an expression for the probability T that electrons, incident from vacuum, reach the metal substrate and contribute to the transmitted current I_t. In the quasielastic scattering regime, this probability depends upon (i) the probability P_{entrance} that incident electrons enter the film, (ii) the angular distribution of electrons after a possible surface scattering at the entrance, (iii) the ratio z of the film thickness L to the electron scattering mean free path λ, (iv) the type of differential cross sections of the bulk scatterings, (v) the reflectivities of the film-vacuum and film-metal interfaces (R_v and R_m, respectively), and (vi) the angular distribution of electrons after reflections at the two interfaces of the film. As shown in I, T can be written as

$$T = P_{\text{entrance}} \left[1 - \frac{P_e(1-R_v)}{1-R_v P_v} \right], \tag{1}$$

where P_i ($i = e$ or v) is given by

 ©1988 The American Physical Society

$$P_i = S_i B_i + \frac{(1-S_i B_i) R_m (1-S_m B_m)}{1-S_m B_m R_m} . \quad (2)$$

Here, S_i is the "scattering probability," i.e., the probability that the electrons which enter the film ($i=e$), or are reflected by an interface ($i=v$ or m), are scattered in the film before reaching the opposite interface. B_i is the "backscattering probability," i.e., the probability that the electrons scattered in the film return, directly or via multiple scattering, and without being reflected by the opposite interface, to the interface (denoted by the subscript i) from which they originated. The evaluation of S_i and B_i is described in detail in I. They both depend upon the "standardized layer thickness" z and the angular distributions of electrons at the entrance of the film and after reflections at the interfaces. B_i also depends on the type of differential cross sections of the bulk scatterings. In this study, we make the usual assumption that bulk scattering is isotropic.

Our analysis of the experimental LEET spectra consists in fitting, for each selected electron energy, the theoretical transmission probability T to the measured values of I_t/I_0 as a function of film thickness. The fits were done with a nonlinear least-squares method, using the algorithm of Marquardt.[22] The errors were estimated on the basis of the residuals and the Hessian matrix.[23]

So far, the unknown parameters involved in the calculation of T are P_{entrance}, λ, R_v, R_m, and the angular distributions. In order to obtain significant results, we must however reduce the number of the adjustable parameters of the model. This is done by making some assumptions concerning the behavior of the electrons at the interfaces of the film. For example, we assume that the film-metal reflectivity, although an unknown quantity, can be approximated by the experimentally measured vacuum-metal reflectivity.[10,13,16] As to the film-vacuum reflectivity, it can be evaluated by means of the Snell-Descartes law.[13,24] According to this law, an injected electron can return to vacuum if it reaches the film-vacuum interface with an angle θ (relative to the surface normal of the film) smaller than the "critical" angle θ_c given by

$$\theta_c = \begin{cases} \arcsin\{[m_0 E/m^*(E+A)]^{1/2}\} & \text{for } A>0 \\ 90^\circ \text{ for } A<0 , \end{cases} \quad (3)$$

where A is the film's electron affinity or, equivalently, the difference in energy between the vacuum level and the bottom of the film's lowest conduction band, m^* is the effective mass of the electron in the film, and m_0 is the free-electron mass. The actual estimation of R_v from the Snell-Descartes law is given in the Appendix.

Having found a way to estimate R_m and R_v, we are now left with only two adjustable parameters, namely, P_{entrance} and λ. These can be determined from a fit of Eq. (1) to the experimental $I_t(E)/I_0$-versus-L data. Regarding the choice of the relevant angular distributions of electrons at the entrance and after reflections from the two interfaces of the film, it is essentially arbitrary since no information is available on this subject in the present literature for the range of electron energies considered here. However, we can use the general expression for the angular distribution $f(\cos^n\theta)$ given in I and compare the results obtained for different values of n. As explained in I, these distributions describe different degrees of forward scattering and involve both the isotropic angular distribution (ISO, $n=0$) and the "direct beam" (DIR, $n\to\infty$) as extreme cases.

IV. RESULTS AND DISCUSSION

For solid xenon films, we analyzed the experimental LEET spectra obtained at a temperature of 45 K with 16 different film thicknesses in the range of 4–500 monolayers.[7,10] Fifty-one electron energies between 1.6 and 7.9 eV were considered independently. The results of the fits are presented in Figs. 1 and 2. These figures show the mean values and the 95% confidence limits of the two estimated parameters, λ and P_{entrance}, as functions of incident electron energy. The confidence intervals were calculated on the basis of Student's t distribution.[25] The fits were all excellent with residuals of about 8×10^{-3} for a range of transmission values varying between 0.03 and 0.3. The films' electron affinity used in the calculations was 0.5 eV for solid xenon,[8,10,12,26] and the electron effective mass was assumed to be equal to the free-electron mass.

In the case of solid molecular nitrogen films, we analyzed the experimental LEET data obtained at 17 K with 7 different overlayer thicknesses, namely, 3, 4, 5.4, 6, 6.8, 10, and 20 monolayers.[16] The fits were performed for 48 different electron energies between 2.4 and 7.4 eV. The values of λ and P_{entrance} obtained from these fits are shown in Figs. 3 and 4 as functions of electron impact en-

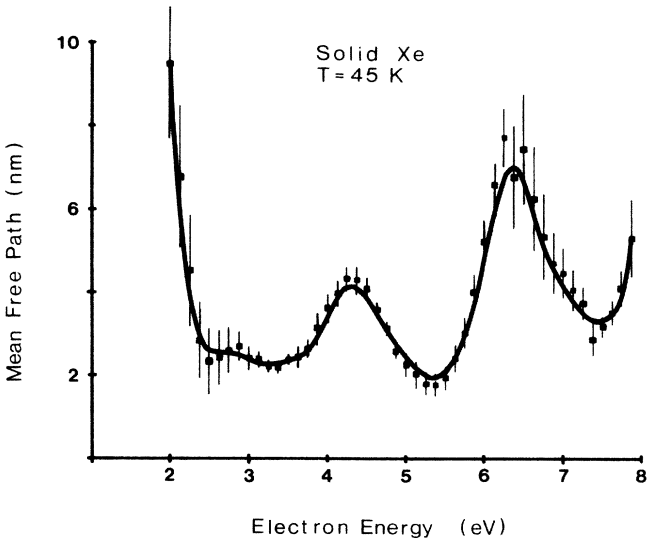

FIG. 1. Energy dependence of the elastic scattering mean free path of excess electrons in solid xenon at 45 K. The solid line is a weighted smoothed curve plotted through the mean values of the least-squares estimates. The error bars show the 95% confidence intervals. The zero of energy is at the vacuum level.

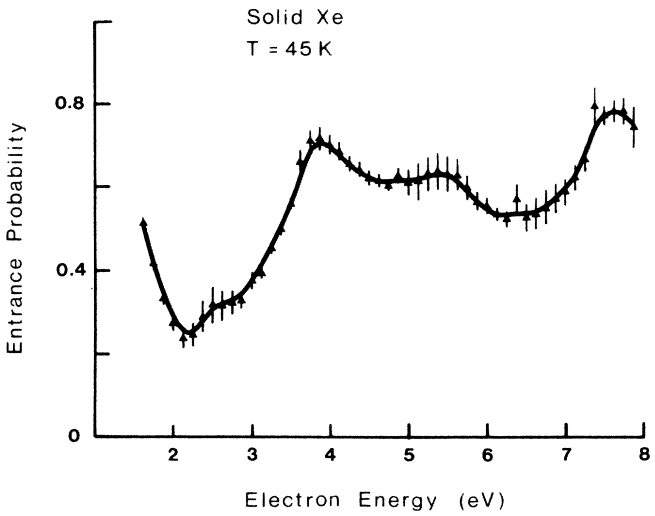

FIG. 2. Entrance probability of incident electrons in solid xenon films at 45 K as a function of electron energy. The solid line is drawn through the mean values of the least-squares estimates of the parameter P_{entrance}. The error bars indicate the 95% confidence limits. The zero of energy is at the vacuum level.

ergy. Again, the fits were excellent with residuals of about 8×10^{-3} for a range of transmission values varying between 0.1 and 0.5. The large uncertainties in the determination of λ at electron energies below 4 eV are due to the lack of experimental data for large film thicknesses. Since the films' electron affinity for solid molecular nitrogen is negative (−0.8 eV),[8] we have taken $R_v=0$. As for solid xenon, m^* was also assumed to be equal to m_0.

Figure 5 shows smoothed curves of the mean values of $\lambda(E)$ in solid xenon obtained for different combinations of electron angular distributions at the entrance to the film and at the two film interfaces. As can be seen from this figure, the choice of the angular distributions can affect

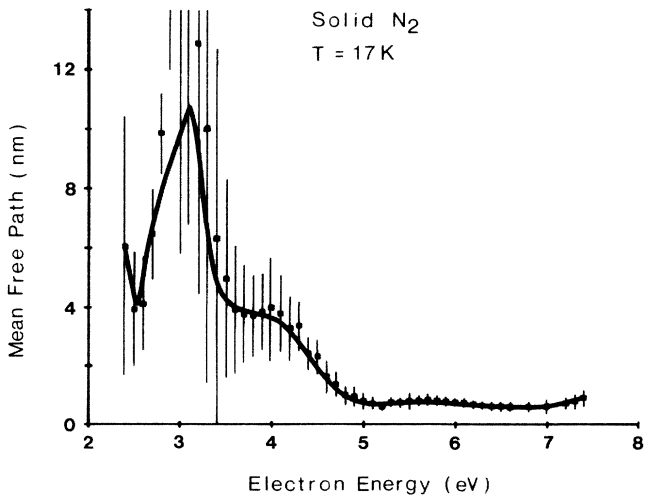

FIG. 3. Same as Fig. 1, for solid molecular nitrogen at 17 K in the quasielastic scattering region.

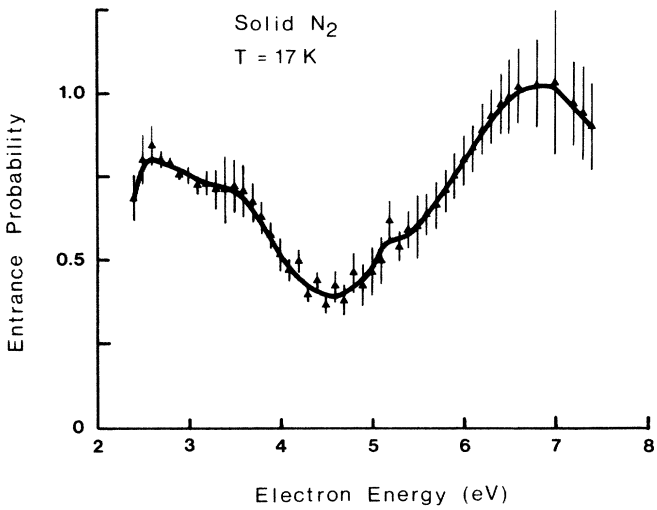

FIG. 4. Same as Fig. 2, for solid molecular nitrogen films at 17 K.

significantly the determination of λ (this is also true for P_{entrance}). The greatest difference observed between results is for the two extreme cases, namely, isotropic scattering (combination eISO-mISO-vISO) and no scattering (combination eDIR-mISO-vISO) of the electrons at the entrance to the film. As expected, the angular distributions used to describe the reflections of electrons at the two film interfaces have a smaller influence on the determination of λ. Unfortunately, the analysis of the variation of the transmitted current with film thickness does not permit us to determine the actual electron angular distributions of the model. In order to minimize the errors due to the choice of the angular distributions,

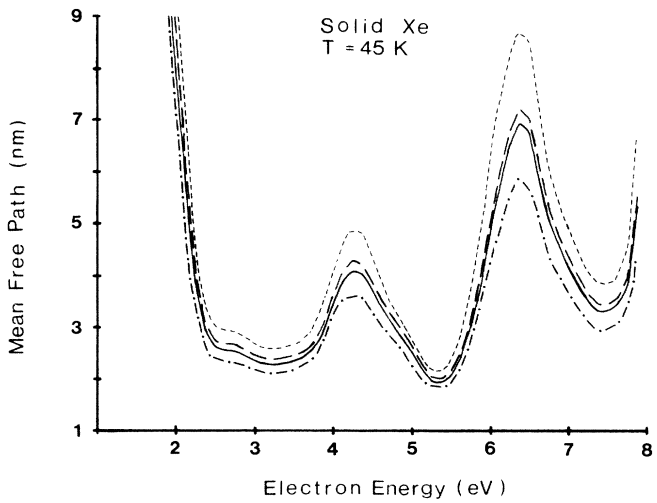

FIG. 5. Comparison of weighted smoothed curves of λ vs E obtained for solid xenon at 45 K by using different combinations of electron angular distributions at the entrance to the film (e), at the film-metal interface (m), and at the film-vacuum interface (v): (- - - - - - -), eISO-mISO-vISO; (— — —), $e\cos^2\theta$-mISO-vISO; (——), $e\cos^2\theta$-$m\cos\theta$-vISO; (—·—·—·), eDIR-mISO-vISO. The symbols ISO, $\cos\theta$, $\cos^2\theta$, and DIR refer to angular distribution functions which were defined in I.

one can use a combination of these which lies between the two extreme cases shown in Fig. 5. For this reason, we chose to present in Figs. 1–4 the results obtained with the combination $e\cos^2\theta$-$m\cos\theta$-vISO. This particular choice seems to be reasonable since the angular distribution of electrons after reflection at the metal boundary is likely to be less directional than that at the entrance to the film. As for the use of an isotropic reflection of electrons at the film-vacuum interface, it is in accordance with the Snell-Descartes law which predicts that most electrons are reflected on this interface with large angles (see Appendix). Of course, more reliable absolute values of P_{entrance} and λ would be obtained if the electron angular distributions of the model could be determined independently.

Figures 6 and 7 show a comparison of various determinations of $\lambda(E)$ in solid xenon at 45 K and solid molecular nitrogen at 17 K, respectively. In these figures, we compare our results with those of Bader *et al.*[7] who used the two-stream approximation, and with those of Plenkiewicz *et al.*[10] and Keszei *et al.*[16] who used a single-scattering model. As we can see, the general variation of λ with E is broadly the same in all cases but its magnitude differs markedly from one study to the other. The advantage of our three-dimensional probabilistic model over the others resides in its ability to handle a wide choice of electron angular distributions without restricting the problem to a single-scattering electron transport formulation. In fact, recent Monte Carlo simulations[19] have shown the significance of including multiple scattering of electrons in the analysis of experimental LEET spectra. In regard to the two-stream method, it is essentially based on a one-dimensional description of electron transport and therefore cannot account for the various electron angular distributions at the film boundaries.

A few words should finally be said about the energy dependence of P_{entrance} and λ for the two studied materials. As can be seen from Figs. 2 and 4, the curves of $P_{\text{entrance}}(E)$ show pronounced structures which can be correlated with the electronic conduction-band density of states of these materials.[8,10,16] Regarding the electron scattering mean free paths (Figs. 1 and 3), large values of λ are observed at incident electron energies below ~ 2 eV for both solids. At higher electron energies ($E > 3$ eV), the curves of $\lambda(E)$ show an oscillatory behavior which can be related to the variation of the electron effective mass with E; a result of the fact that electrons with different energies enter different bands.[27] It is interesting to note that the mean values of both P_{entrance} and λ always show a remarkably smooth and continuous behavior when plotted against electron energy.

V. CONCLUSION

In this paper, we have shown how the model developed in I can be applied to the analysis of experimental LEET data. We have focused our attention on the particular cases of solid xenon and molecular nitrogen but the same kind of analysis can obviously be applied to other systems in the quasielastic scattering region as well. It should also be emphasized that this model can be used to study the transport of other types of particles in solids or gases, other energy ranges, or other kinds of experimental results obtained with plane-parallel media such as reflection spectroscopy or photoemission measurements.

In a subsequent work,[28] we will further develop the general formulation of our model with the introduction of possible inelastic scattering processes which can lower significantly the energy of the particle and therefore affect its transmission probability. This will extend the applicability of the model to the study of a much larger range of experimental results.

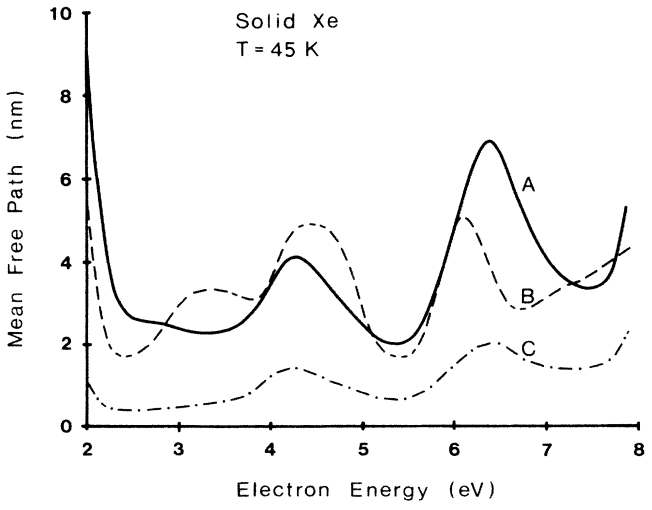

FIG. 6. Comparison of three determinations of $\lambda(E)$ in solid xenon at 45 K: *A*, present work; *B*, Plenkiewicz *et al.* (Ref. 10); *C*, Bader *et al.* (Ref. 7). Note that the $\lambda(E)$ values obtained in Ref. 7 have been multiplied by a factor 0.574 to account for the correct (111) interlayer spacing (0.354 nm) of the physisorbed solid xenon films.

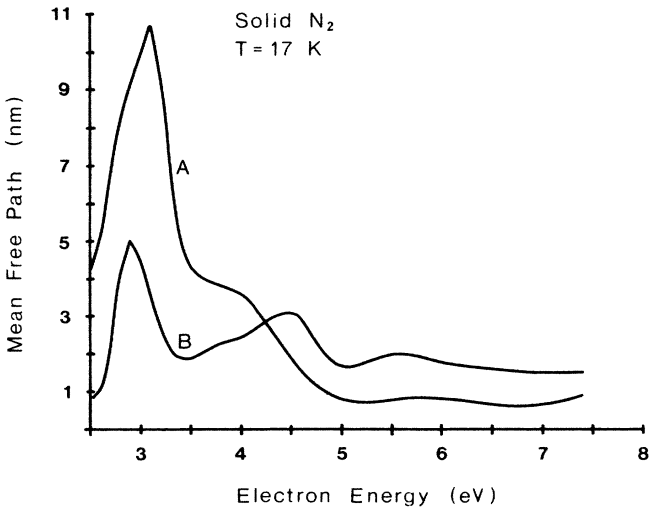

FIG. 7. Same as Fig. 6, for solid molecular nitrogen at 17 K: *A*, present work; *B*, Keszei *et al.* (Ref. 16).

ACKNOWLEDGMENTS

This work was supported by the Medical Research Council of Canada, the Fonds de la Recherche en Santé du Québec, the Natural Sciences and Engineering Research Council of Canada, and the Ministère de l'Enseignement Supérieur et de la Science du Québec. This support is herewith gratefully acknowledged.

APPENDIX

Estimation of R_v using the Snell-Descartes law

Consider an electron which is subjected to an isotropic collision in a plane-parallel film at a distance r from the film-vacuum interface. Its probability of being scattered with a polar angle between θ and $\theta+d\theta$ is given by $\frac{1}{2}\sin\theta\, d\theta$, and the distance it must travel to reach the interface with this angle is $r/\cos\theta$. Under these conditions, the probability for this electron to reach the film-vacuum interface with a polar angle between θ and $\theta+d\theta$ is

$$dP(\theta,r)=\int_{r/\cos\theta}^{\infty}\frac{1}{2\lambda}\sin\theta\exp(-u/\lambda)du\, d\theta \tag{A1}$$

$$=\tfrac{1}{2}\sin\theta\exp(-r/\lambda\cos\theta)d\theta\ . \tag{A2}$$

In order to find the angular distribution of all the electrons which reach this interface, we integrate $dP(\theta,r)$ over r, taking into account the depth distribution of collision sites inside the film. The simplest case is a uniform distribution between $r=0$ and $r=L$ (where L is the film thickness), given by $D(r)=r/L$. In this case, we find[19]

$$dP(\theta)=\frac{1}{2z}\sin\theta\cos\theta[1-\exp(-z/\cos\theta)]d\theta\ , \tag{A3}$$

where $z=L/\lambda$. According to the Snell-Descartes law, the reflectivity of the film-vacuum interface, R_v^f, for the electrons arriving from the film is simply given by the fraction of them which reach this interface with an angle $\theta>\theta_c$. Therefore, we have

$$R_v^f=\frac{\int_{\theta_c}^{\pi/2}dP(\theta)}{\int_0^{\pi/2}dP(\theta)}\ , \tag{A4}$$

which gives, after integration,

$$R_v^f=\{\sin^2\theta_c-(e^{-z}-\cos^2\theta_c e^{-z/\cos\theta_c})-z(\cos\theta_c e^{-z/\cos\theta_c}-e^{-z})-z^2[E_1(z)-E_1(z/\cos\theta_c)]\}/[1-e^{-z}+ze^{-z}-z^2E_1(z)]\ , \tag{A5}$$

where the function $E_1(z)$ is the exponential integral defined as

$$E_1(z)=\int_1^{\infty}\frac{e^{-zt}}{t}dt\ . \tag{A6}$$

It is interesting to note that in the limit $z\to 0$, $R_v^f\to\cos\theta_c$, which is equivalent to the expression used by Bader and co-workers [see Eq. (5) of Ref. 7] for all values of z in their analysis of LEET spectra of solid xenon films. For large values of z, R_v^f is found to be smaller since the electrons tend to reach the film-vacuum boundary with small angles θ.

Let us now consider the reflectivity of the film-vacuum interface, R_v^m, for the electrons which reach this interface directly after reflection by the metal, that is, without scattering in the film. These electrons are at a distance L from vacuum and leave the film-metal boundary with an angular distribution $f(\theta)$. Their probability to reach the film-vacuum interface with a polar angle between θ and $\theta+d\theta$ is

$$dP(\theta,L)=f(\theta)\exp(-L/\lambda\cos\theta)d\theta\ . \tag{A7}$$

Again, according to the Snell-Descartes law, we have

$$R_v^m=\frac{\int_{\theta_c}^{\pi/2}dP(\theta,L)}{\int_0^{\pi/2}dP(\theta,L)}\ . \tag{A8}$$

For the case of a semi-isotropic angular distribution of electrons reflected at the metal boundary, we have $f(\theta)=\sin\theta$ and the integration of Eq. (A8) yields

$$R_v^m=\frac{\cos\theta_c e^{-z/\cos\theta_c}-zE_1(z/\cos\theta_c)}{e^{-z}-zE_1(z)}\ . \tag{A9}$$

The calculation of R_v^m can also be performed for other angular distributions of reflected electrons. For example, if we have $f(\theta)=2\sin\theta\cos\theta$, we obtain

$$R_v^m=\frac{\cos^2\theta_c e^{-z/\cos\theta_c}-z\cos\theta_c e^{-z/\cos\theta_c}+z^2E_1(z/\cos\theta_c)}{e^{-z}-ze^{-z}+z^2E_1(z)}\ . \tag{A10}$$

Obviously, the global reflectivity of the film-vacuum interface, R_v, is somewhere between R_v^f and R_v^m. In order to determine R_v, the relative proportions of electrons arriving at the film-vacuum interface, either from the film or directly from the metal, must be evaluated. The probability that the electrons arrive on this interface from the film is

$$K_f=S_eB_e+[1-S_e+S_e(1-B_e)]R_mS_m(1-B_m)\times\sum_{n=0}^{\infty}(B_mR_mS_m)^n\ . \tag{A11}$$

Since the product $(B_mR_mS_m)$ is smaller than 1, the infinite series in Eq. (A11) can be summed and has the

value $1/(1-B_m R_m S_m)$, whence

$$K_f = S_e B_e + \frac{(1-S_e B_e) R_m S_m (1-B_m)}{1-B_m R_m S_m} . \quad \text{(A12)}$$

Similarly, the probability that the electrons arrive on the film-vacuum interface directly from the metal is

$$K_m = [1-S_e+S_e(1-B_e)] R_m (1-S_m) \sum_{n=0}^{\infty} (B_m R_m S_m)^n , \quad \text{(A13)}$$

which reduces to

$$K_m = \frac{(1-S_e B_e) R_m (1-S_m)}{1-B_m R_m S_m} . \quad \text{(A14)}$$

The global expression for R_v can then be written as follows:

$$R_v = \frac{K_f R_v^f + K_m R_v^m}{K_f + K_m} . \quad \text{(A15)}$$

This whole derivation might seem overly lengthy but recent Monte Carlo calculations[29] have shown that taking simpler expressions for R_v, such as $\cos\theta_c$ or R_v^f alone, can lead to non-negligible systematic errors in the determination of the electron scattering mean free paths.

---

*Permanent address: Department of Physical Chemistry and Radiology, L. Eötvös University, Puskin u. 11-13, H-1088 Budapest, Hungary.

†Also at the Centre de Recherche en Physique du Solide, Département de Physique, Faculté des Sciences, Université de Sherbrooke, Sherbrooke, Québec, Canada J1K 2R1.

[1]T. Goulet, E. Keszei, and J.-P. Jay-Gerin, preceding paper, Phys. Rev A **37**, 2176 (1988), paper I of this series.

[2]K. Hiraoka and W. H. Hamill, J. Chem. Phys. **57**, 3870 (1972); **59**, 5749 (1973).

[3]M. E. Harrigan and H. J. Lee, J. Chem. Phys. **60**, 4909 (1974).

[4]S. C. Dahlberg, Phys. Rev. B **19**, 5369 (1979).

[5]L. Sanche, J. Chem. Phys. **71**, 4860 (1979); L. Sanche, G. Bader, and L. Caron, *ibid.* **76**, 4016 (1982).

[6]K. Hiraoka, J. Phys. Chem. **85**, 4008 (1981); K. Hiraoka and M. Nara, *ibid.* **86**, 442 (1982); Chem. Phys. Lett. **94**, 589 (1983).

[7]G. Bader, G. Perluzzo, L. G. Caron, and L. Sanche, Phys. Rev. B **26**, 6019 (1982).

[8]G. Bader, G. Perluzzo, L. G. Caron, and L. Sanche, Phys. Rev. B **30**, 78 (1984).

[9]G. Perluzzo, L. Sanche, C. Gaubert, and R. Baudoing, Phys. Rev. B **30**, 4292 (1984); G. Perluzzo, G. Bader, L. G. Caron, and L. Sanche, Phys. Rev. Lett. **55**, 545 (1985).

[10]B. Plenkiewicz, P. Plenkiewicz, G. Perluzzo, and J.-P. Jay-Gerin, Phys. Rev. B **32**, 1253 (1985).

[11]J.-P. Jay-Gerin, B. Plenkiewicz, P. Plenkiewicz, G. Perluzzo, and L. Sanche, Solid State Commun. **55**, 1115 (1985); P. Plenkiewicz, J.-P. Jay-Gerin, B. Plenkiewicz, and G. Perluzzo, *ibid.* **57**, 203 (1986).

[12]L. Sanche, G. Perluzzo, and M. Michaud, J. Chem. Phys. **83**, 3837 (1985).

[13]T. Goulet and J.-P. Jay-Gerin, Radiat. Phys. Chem. **27**, 229 (1986).

[14]L. G. Caron, G. Perluzzo, G. Bader, and L. Sanche, Phys. Rev. B **33**, 3027 (1986).

[15]N. Ueno, K. Sugita, K. Seki, and H. Inokuchi, Phys. Rev. B **34**, 6386 (1986).

[16]E. Keszei, J.-P. Jay-Gerin, G. Perluzzo, and L. Sanche, J. Chem. Phys. **85**, 7396 (1986).

[17]R. M. Marsolais, M. Michaud, and L. Sanche, Phys. Rev. A **35**, 607 (1987).

[18]U. Fano, Phys. Rev. A **36**, 1929 (1987).

[19]T. Goulet, J.-P. Jay-Gerin, and J. P. Patau, J. Electron Spectrosc. Relat. Phenom. **43**, 17 (1987).

[20]G. Leclerc, T. Goulet, P. Cloutier, J.-P. Jay-Gerin, and L. Sanche, J. Phys. Chem. **91**, 4999 (1987).

[21]T. Goulet, E. Keszei, and J.-P. Jay-Gerin, in *Proceedings of the Sixth Tihany Symposium on Radiation Chemistry, Balatonszéplak, Hungary, 1986,* edited by P. Hedvig, L. Nyikos, and R. Schiller (Akadémiai Kiadó, Budapest, 1987), p. 75.

[22]D. W. Marquardt, J. Soc. Indust. Appl. Math. **11**, 431 (1963).

[23]See, for example, W. H. Press, B. P. Flannery, S. A. Teukolsky, and W. T. Vetterling, *Numerical Recipes: The Art of Scientific Computing* (Cambridge University Press, Cambridge, 1986), p. 521.

[24]See, for example, J. D. Jackson, *Classical Electrodynamics* (Wiley, New York, 1975), p. 278; M. Rei Vilar, Thèse de Doctorat ès-Sciences Physiques, Université Paris VII, Paris, 1985.

[25]See, for example, J. Mandel, *The Statistical Analysis of Experimental Data* (Dover, New York, 1964), p. 114.

[26]N. Schwentner, F.-J. Himpsel, V. Saile, M. Skibowski, W. Steinmann, and E. E. Koch, Phys. Rev. Lett. **34**, 528 (1975); J. Jortner and A. Gaathon, Can. J. Chem. **55**, 1801 (1977); W. von Zdrojewski, J. G. Rabe, and W. F. Schmidt, Z. Naturforsch. **35a**, 672 (1980).

[27]B. Plenkiewicz, P. Plenkiewicz, and J.-P. Jay-Gerin, Phys. Rev. B **33**, 5744 (1986).

[28]T. Goulet, E. Keszei, and J.-P. Jay-Gerin [paper III of this series (unpublished)].

[29]T. Goulet (unpublished).